Proximity effect in a superconductor/exchange-spring-magnet hybrid system

J. Y. Gu[*] and Jefery Kusnadi

Department of Physics and Astronomy, California State University–Long Beach, Long Beach, California 90840, USA

Chun-Yeol You[†]

Department of Physics, Inha University, Incheon 402-751, Korea

We investigate the proximity effect in a superconductor/ferromagnet (S/F) hybrid system with a noncollinear magnetic configuration. A new structure of an S/exchange-spring (ES) magnet is fabricated, where an ES magnet is employed as an F layer since the magnetization configuration is varied from a collinear state to a noncollinear state by a rotating external magnetic field in a well controllable way. We found that the resistance decreases and the superconducting transition temperature increases, as noncollinearity is introduced starting from a collinear state. We interpret that our experimental observation is due to the contribution of the odd-triplet superconducting condensate that survived in a noncollinear magnetization configuration in the ES magnet.

I. INTRODUCTION

Superconductor/ferromagnet (S/F) hybrid structures show exotic phenomena such as proximity effect, inverse proximity effect, triplet superconductivity, π junctions, domain-wall superconductivity (DWS), etc.[1,2] One of the most interesting observations is the proximity effect. A superconducting order parameter is suppressed due to the F layer and thus superconducting transition temperature, T_c, decreases or oscillates.[3,4] A simple physical interpretation of the proximity effect is that the Cooper pairs are broken by a strong exchange coupling field in the F layer, where parallel spins are preferred.

The so-called *superconducting spin-switch* effect is a marvelous phenomenon related to the proximity effect found in the F/S/F trilayer structures.[5–10] It manifests itself by the existence of nonzero $\Delta T_c = T_c^{AP} - T_c^{P}$, where $T_c^{P,AP}$ stand for the T_c of parallel and antiparallel magnetization configurations of the two F layers, respectively. In a simple argument of proximity effect, nonzero ΔT_c is ascribed to the different effective exchange fields between the P and AP configurations. The pair breaking by the proximity effect in the AP configuration is weaker since the exchange fields from two F layers are canceled each other to cause $T_c^{AP} > T_c^{P}$. However, experimental observations are still controversial since there were observations for the opposite case, $T_c^{AP} < T_c^{P}$.[11–13]

Another interesting phenomenon in S/F system, which only shows up under a specific magnetic environment, is an odd-triplet superconductivity. Different types of superconducting condensate have been observed in various superconducting systems. Singlet pairing observed in most of conventional low T_c (s-wave singlet) and high-T_c cuprates (d-wave singlet) superconductors showed that the symmetric part of the condensate function is an even function of the Matsubara frequency, ω. Another type of pairing, spin-triplet superconducting condensate of two electrons with the same spin, has been discovered in several systems, such as, UPt$_3$,[14] Sr$_2$RuO$_4$,[15,16] and Bechgaard salts, (TMTSF)$_2$PF$_6$.[17] For the conventional spin-triplet superconductivity present in the above examples, the symmetric part of condensate function is even in frequency and odd in momentum as same as the singlet one. Conventional spin-triplet pairing is very sensitive to the impurity concentration.

Recently, new type of superconducting condensate with triplet pairing was reported in S/F systems.[9,18–22] This pairing is called odd-triplet superconductivity since it is odd in frequency and even in momentum. Since the triple condensate has the parallel spin configurations the triplet superconducting state is not sensitive to the existence of the ferromagnet exchange field.[19] Although the odd-triplet condensate survives in the presence of a strong impurity scattering the components of $S_z = 0$ and $S_z = \pm 1$ in triplet pairing have different characteristics. In case of the homogeneous magnetization in F layer only a component with total projection $S_z = 0$ arises alongside with the conventional singlet condensate. This component decays rapidly as a length scale of ξ_S in dirty limit, which is similar to the singlet one. The decay length ξ_S in a homogeneous F layer is given by $\sqrt{D_F/h}$, where D_F and h are diffusion constant and exchange energy of the F layer, respectively. However, for inhomogeneous magnetization in F layer, all the components of triplet condensate are available alongside with the singlet one. In the diffusive limit, the amplitude of symmetric component with $S_z = \pm 1$ dominates and this component penetrates F layer over a long distance in a length scale of $\xi_T = \sqrt{D_F/2\pi T}$. ξ_T is much longer than ξ_S since $2\pi T \ll h$. It is similar to the nonmagnetic material case.[19,23,24]

The slow decaying triplet condensate leads a large Josephson effect[25–28] and DWS.[29] After DWS was first observed by Yang *et al.*,[30] DWS-related phenomena were theoretically predicted[29,31,32] and experimentally found in various systems, such as, Py (=Ni$_{80}$Fe$_{20}$)/Nb bilayer[33] and [Co/Pt]$_N$/Nb/[Co/Pt]$_N$ multilayer systems.[34] They found the enhancement of superconducting state when the magnetic layer forms multidomain structure. At the vicinity of the domain wall, where the magnetizations are inhomogeneous, an effective exchange field gets weaker and the average exchange field experienced by Cooper pairs within a coherence
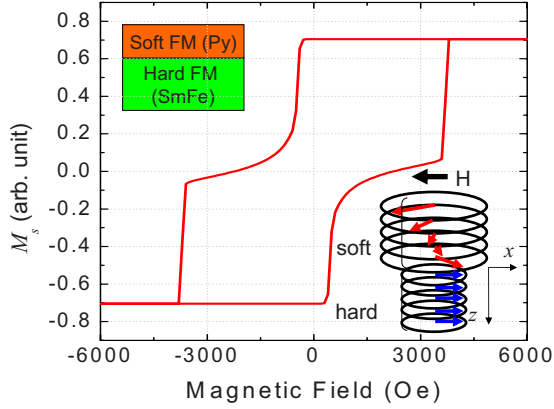
FIG. 1. (Color online) A typical hysteresis loop of an ES magnet. (Insets) A typical structure and a schematic image of the magnetization configuration of an exchange-spring magnet.

length becomes smaller. However, in most of the above structures, it was difficult to control the domain structures. Therefore, if we can generate and control the inhomogeneity (noncollinearity) in the magnetization of the F layer near the S/F interface, we will experimentally observe the contribution of odd-triplet component in a controllable way.

In this study, we employed a hybrid structure of a superconductor and an exchange-spring (ES) magnet (hereafter we call it "S/ES hybrid system"), Nb/Py/SmFe, to investigate the proximity effect under a noncollinear magnetization configuration. The magnetization configuration of an ES magnet near the S/F interface was varied from a collinear state to a noncollinear state by rotating an external magnetic field, H_{ext}. Resistance, R, measured while rotating H_{ext}, showed that the T_c increases by establishing the noncollinearity in the magnetizations of the F layer. We interpret that the observed T_c enhancement is due to the contribution of the odd triplet condensates in the vicinity of noncollinear magnetization configuration.[2,23]

II. EXPERIMENTAL DETAILS

Figure 1 shows a typical magnetic hysteresis loop of an ES magnet. The ES magnet consists of the two F layers, hard (SmFe) and soft (Py) layers as shown in the inset of Fig. 1.[35–37] The magnetization reversal process in ES magnet can be simulated by a calculation with a simple atomic layer model where the bilayers and the multilayers are composed of stacking of atomic layers. In an ES magnet, the soft layer is tightly coupled to the hard layer due to the strong interface exchange coupling between the two layers. If soft layer thickness is larger than the domain-wall width, the bottom part of the soft layer is strongly pinned at the interface but the topmost part of the soft layer is almost free to rotate with an external magnetic field. The angle between each magnetization and the magnetization of the hard layer increases with increasing distance from the hard layer, resulting in a spiral spin structure similar to that in a Bloch domain wall. This continuously changing spiral spin structure introduces a noncollinear magnetization configuration as shown in the inset of Fig. 1. Therefore, the S/ES hybrid system is an ideal

system that can be used to study the proximity effect of S/F system due to a noncollinear magnetic configuration. Furthermore, the noncollinearity in ES can be controlled by the strength or direction of the external magnetic field.

An S/ES structure, Nb(30 nm)/Py(19)/SmFe(35), was deposited on Si substrates using a sputtering system. Details of the sample preparation are reported elsewhere.[38] Magnetization was measured using a vibrating sample magnetometer of a Quantum Design physical property measurement system (PPMS-9T). The horizontal rotator option of PPMS was used to measure $R(\theta)$ while rotating the sample. Here θ is the angle between H_{ext} and the magnetization of the hard layer. External magnetic field was always applied in plane of the thin-film sample with varying θ. A schematic of the experimental setup for the sample rotation is shown in Fig. 2(a).

III. RESULTS AND DISCUSSION

A. Magnetic configuration

First, we applied a large enough external magnetic field (H_{ext}=2 T) parallel to the x axis (magnetization direction of the hard layer, $\theta=0°$) in order to saturate the soft and hard layers. After that, H_{ext} was reduced to a moderate field (100–2000 Oe) and the sample was rotated with an angle θ. Rotating the sample is equivalent to rotating H_{ext}. Therefore, in this study we refer to "rotating H_{ext}" instead of "rotating sample." Current was always applied parallel to the x axis.

Before we discuss the result of $R(\theta)$, we need to figure out the magnetization configuration established in the F layer by rotating H_{ext}. Figure 2(b) illustrates the magnetization configuration of ES magnet for a rotating field, where it shows a noncollinear magnetization along the z axis in the soft layer. In Fig. 2(c), we depicted the simulated result of ϕ_i for each ith layer[35] using a representative example of H_{ext}=2000 Oe. ϕ_i is the angle between the magnetization of the ith layer and x axis. Dotted vertical lines correspond to the interfaces of the S/ES and the soft/hard layers. The interface between the S and ES is marked as $i=0$.

Since the H_{ext} (=2000 Oe) is much smaller than the coercivity of the hard layer ($H_c \sim 3$ T at $T \sim 5$ K), the magnetization orientation of the hard layer is considered not to change. For $\theta=0°$, both layers are saturated (all $\phi_i=0°$). Rotating H_{ext} drags the topmost soft layer magnetization ($i \approx 0$) while the magnetization of the bottom soft layer ($i \approx 100$) is pinned along the hard layer magnetization. ϕ_i of the topmost layer is close to θ when H_{ext} is large enough but it is always smaller than θ.

Figures 2(d)–2(f) show some of the ϕ_i's in different θ regimes. Figure 2(d) is for a small value of θ, where ϕ_i changes continuously to generate a noncollinear magnetization configuration. The blue, red, and green arrows represent top, middle, and bottom magnetizations of the soft layer, respectively. The black thin arrows are H_{ext}. When θ exceeds a critical value (>270° in our simulation) there are two possible configurations as shown in Figs. 2(e) and 2(f). Configuration II requires large amount of interatomic exchange energy due to the large deviation angle between the adjacent layers. Therefore, ϕ_i's reconfigure to the configuration III, where the system total energy is minimized since the de-
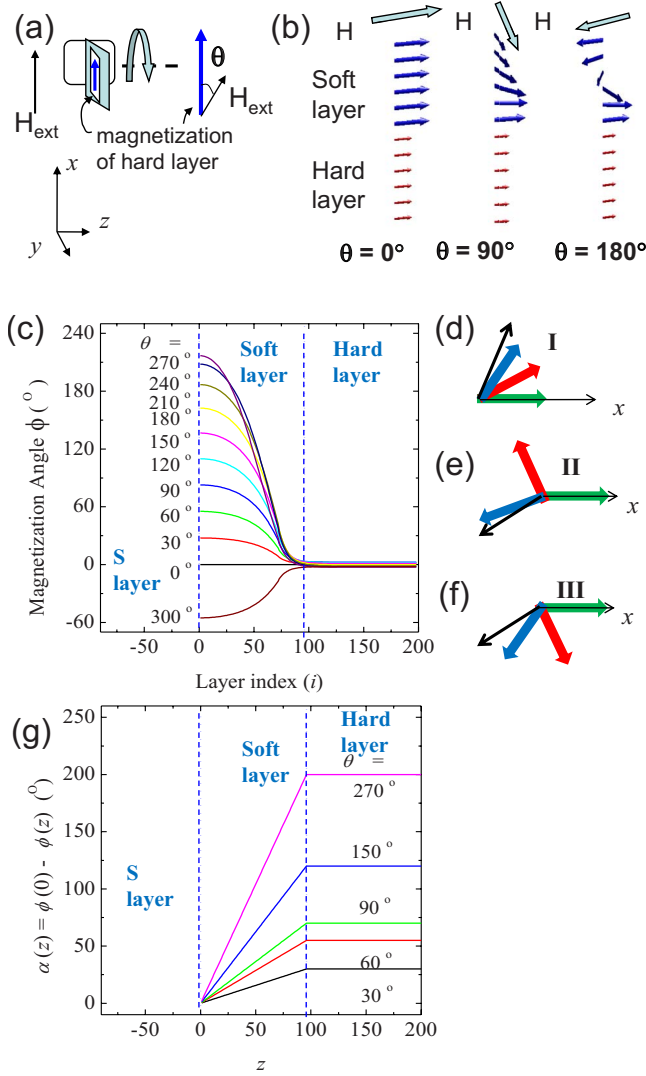
FIG. 2. (Color online) (a) A schematic of the experimental setup of rotation experiment. (b) Illustrations of the magnetization configurations of an ES magnet with a rotating magnetic field. (c) Simulation of the distribution of magnetization angle ϕ_i for each ith layer using a representative example of $H_{ext}=2000$ Oe. Blue dashed lines correspond to the interfaces of superconductor/soft layer and soft/hard layers. (d) Configuration I corresponds to a small value of θ. Configurations II (e) and III (f) show two possible magnetization configurations for the value of θ larger than a critical angle ($\theta > 270°$). The blue, red, and green arrows represent the top, middle, and bottom magnetizations of the soft layer, respectively. The black thin arrows are H_{ext}. (g) $\alpha(z) = \phi(0) - \phi(z)$ from the simulation results of (c) with linear approximation.

crease in the interatomic exchange energy by reducing the deviation angle between the adjacent layers is larger than the increase in the Zeeman energy term. As a result, in the high θ regime, the actual state is expected to form mixed states of II and III, so the monodomain model is no longer valid. The critical angle and the details of ϕ_i's should depend on the magnitude of H_{ext}. A larger critical angle is expected for a larger H_{ext}. Our simulation result suggests that rotating H_{ext} introduces a noncollinear magnetization configuration in a
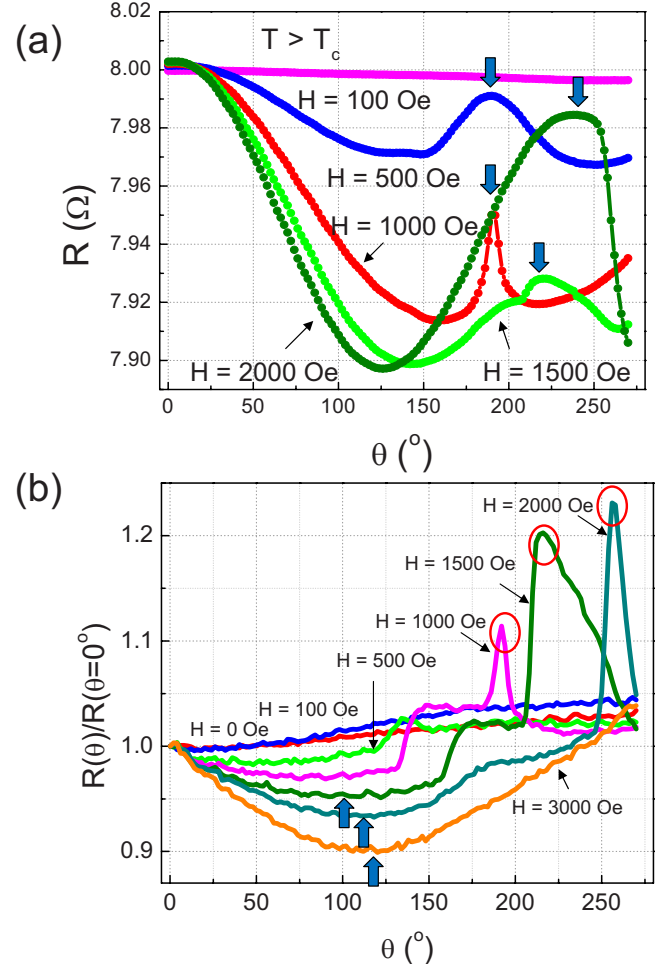

FIG. 3. (Color online) (a) AMR as a function of θ for various H_{ext} (=100, 500, 1000, 1500, and 2000 Oe) at 4.5 K ($>T_c$). (b) Normalized resistance, $R(\theta)/R(\theta=0)$, as a function of θ for various H_{ext} (=0, 100, 500, 1000, 1500, 2000, and 3000 Oe) at 3.23 K ($\sim T_c$).

controllable and reliable way within a certain range of θ which depends on the magnitude of H_{ext}.

B. Transport properties

Figures 3(a) and 3(b) show $R(\theta)$ of Nb/Py/SmFe/Si measured at $T=4.5$ K $> T_c$ and $T=3.23$ K $\sim T_c$ with various H_{ext} values, respectively. $R(\theta)$ measurement has an advantage over a typical magnetoresistance (MR) measurement, $R(H_{ext})$. A noncollinear magnetization configuration can be obtained in both measurements, but the one in the $R(H_{ext})$ measurement occurs near the switching field regime, where a multidomain formation occurs due to the polycrystalline nature of our sample. Since the stray fields from the multidomain formation dominate the proximity effect, the contribution from the noncollinearity is neglected. However, in a rotating field measurement, $R(\theta)$, we can introduce a noncollinearity without being disturbed by stray fields unless θ exceeds the critical angle.

In Fig. 3(a), $R(\theta)$ in normal state can be ascribed to the anisotropic MR (AMR) of the Py layer.[39] According to the

magnetization configurations in Fig. 2(c) and the nature of AMR, the H_{ext} and θ dependence of AMR in Fig. 3(a) is qualitatively understandable. The measured AMR in Fig. 3(a) is approximately expressed as $R(H_{ext}, \theta) \sim \langle R_0 \rangle - \langle \Delta R_i \rangle \sin^2 \langle \phi_i \rangle$, where $\Delta R_i (>0)$ is the magnitude of the MR of each ith layer and $\langle \ \rangle$ is the weighted average values over the whole F layers with the assumption of the current in plane.[39]

For a given H_{ext}, $\langle \phi_i \rangle$ increases with increasing θ, and thus R decreases due to the $\sin^2 \langle \phi_i \rangle$ dependence of AMR. As H_{ext} increases, a larger AMR value (due to $\langle \phi_i \rangle$) is obtained for a given θ as shown in Fig. 3(a). At $\langle \phi_i \rangle \sim 90°$, $R(\theta)$ shows a minimum and increases again for $\langle \phi_i \rangle > 90°$. However, if θ exceeds some critical values, as indicated by vertical blue arrows in Fig. 3(a), the simple monodomain model is not valid and $\sin^2 \langle \phi_i \rangle$ dependence is broken. The maximum AMR in our measurements is about 1.25%, which well agrees to the typical AMR value of Py.[39] Experimental AMR data in Fig. 3(a) and the simulation result in Fig. 2(c) suggest that our S/ES system indeed provided a well-defined noncollinear magnetizations near the S/ES interface by rotating H_{ext}.

Before we discuss experimentally observed $R(\theta)$ of the S/ES system at $T \sim T_c$ shown in Fig. 3(b), let us briefly explain the related theories. According to previous theoretical works,[9,19–21] only singlet condensate can exist in isolated S layer in the dirty limit. Triplet condensate becomes available for the S/F bilayers. For the homogeneous F layer, only the component of $S_z=0$ projection has nonzero values but the other component of $S_z= \pm 1$, odd triplet, can not exist. When the magnetic configurations are noncollinear, the odd-triplet components of $S_z= \pm 1$ are no longer zero. The component of $S_z=0$ decays rapidly, but the components of $S_z= \pm 1$, dominating in the inhomogeneous F layer, penetrate F layer over a long distance. The triplet components do not explicitly appear in the self-consistency equation,[20,21,40–42] however, the triplet contributions must be taken into account to obtain correct T_c. Since the triplet condensate is coupled with singlet one through the complementary boundary conditions, the nonzero odd-triplet condensate will change the T_c of the S/ES system.

Bergeret *et al.*[2,23] found an analytic relationship between the amplitude of the odd-triplet component and the distribution of magnetization vectors in the F layer [see Eq. (3.60) in Ref. 2]. For the S/ES system, the angle of magnetization in F layer (soft layer) changes continuously along the vertical direction to the S/F interface as already shown in Fig. 2(c). To compare our experimental data with theoretical work[2] we define the angle of the magnetization in F layer relative to the magnetization at the S/F interface as α, $\alpha(z) = \phi(z=0) - \phi(z)$. We assume, for simplicity, that α has a simple relationship with the depth from the interface, z; $\alpha(z) = Qz$ ($0 < z < w$) and $\alpha(z) = \alpha_w$ ($z > w$), where z, Q, w, and α_w are the depth from the interface which is proportional to the layer index i, slope of the magnetization variation to the z direction, domain-wall width, and the maximum angle, respectively.[2] This means that the magnetization vector is aligned parallel to the external magnetic field [$\alpha(0)=0°$] at the S/F interface and rotates by $\alpha(z)=Qz$ within the length scale of domain-wall width. At $z > w$ the orientation of the

magnetization is fixed (at the soft/hard interface, the magnetization is fixed along the magnetization of the hard layer).

The schematic behavior of $\alpha(z)$ for various θ are depicted in Fig. 2(g) based on the simulation results in Fig. 2(c) with linear approximation. When we look at Fig. 2(g), Q and the maximum angle of ϕ increase with θ indicating that the amplitude of the odd-triplet component is tuned in S/ES system by rotating H_{ext}. We can roughly say Q increases monotonically with θ. They found that there is no triplet excitation for the collinear magnetization configuration, $Q=0$. When Q (or θ) increases the triplet amplitude increases from zero, reaches its maximum value at a certain Q_{max}, and then decreases (see Fig. 11 of Ref. 2).

Figure 3(b) shows the central experimental result of our work, the normalized resistance, $R(\theta)/R(\theta=0)$, of Nb/Py/SmFe/Si as a function of θ for various H_{ext} (=0, 100, 500, 1000, 1500, 2000, and 3000 Oe) at 3.23 K ($\sim T_c$). First, let us focus only on the $0° < \theta < 120°$ region for $H_{ext} > 500$ Oe. It clearly shows that R decreases by rotating H_{ext}. $R(\theta)$ variation can be interpreted with aforementioned theories. With a rotating H_{ext}, ϕ_i starts to evolve as shown in Fig. 2(c) and Q also increases from 0. Nonzero Q implies that the configuration of a noncollinear magnetization is formed in the soft layer and causes nonzero magnitude of the odd-triplet condensate at the interface. As a result, we observed a decrease in R or an increase in T_c.

As aforementioned, when Q reaches Q_{max} at a certain value of θ for a given H_{ext}, the magnitude of odd-triplet condensate has its maximum value. After that, increasing θ leads a decrease in T_c. Therefore, the observed minima in R, marked with the blue vertical arrows in Fig. 3(b), indicate the points of $Q=Q_{max}$. Since the Q and α_w are a function of H_{ext} and θ, the details of $R(\theta)$, such as its minima, are also the function of H_{ext}.

The functional form of $R(H_{ext}, \theta)$ has not been obtained yet. In Fig. 2(g), we simulated the magnetization configuration using the linear approximation of $\alpha(z)$ employed in the theory.[2] However, the actual configuration of magnetization will probably be different from the linear approximation when both H_{ext} and θ are involved simultaneously. More quantitative analysis of $R(\theta)$ for different H_{ext} requires further theoretical study and independent measurement of vertical magnetization configuration, $\alpha(z)$, as a function of both H_{ext} and θ, which are beyond the scope of our current work.

For larger values of θ, we observed a peak in $R(\theta)$ curve as indicated with red circles in Fig. 3(b). The position of the peak is shifted toward higher angles for larger H_{ext}. We conjecture that the abnormal increase in R at higher angles is due to the strong stray fields that were generated from the formation of multidomain states in ES layer, which then penetrated into the S layer. Near T_c the critical field of the S layer is very small and thus some parts of the S layer become normal state or vortexes are formed due to the stray field. As a result, the large increase in R was observed as shown in Fig. 3(b).

Based on the theoretical calculation[2] and our experimental observation, we can conjecture that rapid change in the magnetization (large Q) within the length scale of the penetration length from the S/ES interface leads T_c increment and it can be explained with the excitation of the triplet condensate. However, if the change is too fast, the change in T_c de-
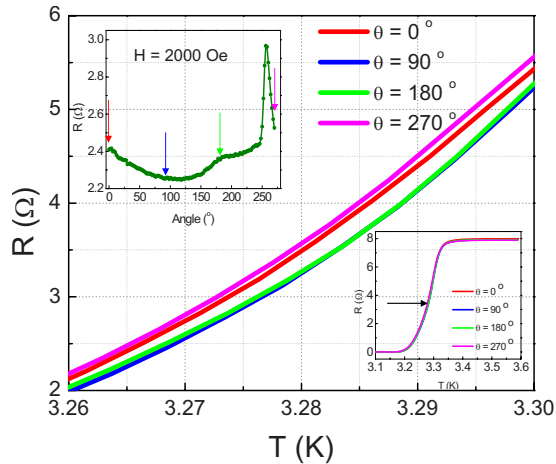
FIG. 4. (Color online) $R(T)$ of the S/ES hybrid system with various θ values, $\theta = 0°$, $90°$, $180°$, and $270°$ with $H_{ext} = 2000$ Oe. (Insets) $R(T)$ in a whole temperature range and $R(\theta)$ graph at $T = 3.4$ K with $H_{ext} = 2000$ Oe.

creases. For example, the proximity effect of the antiferromagnet can be treated as a nonmagnet.[43,44]

We have to emphasize that the singlet condensate and triplet condensate with the projection $S_z = 0$ can not play an important role in our observation of $R(\theta)$ due to their short penetration length, only a few atomic monolayers. In this length scale, the change in ϕ_i is almost negligible and the F layer is considered homogeneous during the field rotation. Therefore, their contribution to the change in T_c as a function of θ is negligible in our experiments, where $1/Q$ is the order of soft layer thickness, 19 nm. However, the long-range odd-triplet component generated by noncollinear magnetic configuration experiences a huge change in ϕ_i throughout the entire soft magnetic layer and makes a major contribution to the R (or T_c) dependence on θ.

In Fig. 4, we plotted $R(T)$ for $\theta = 0°$, $90°$, $180°$, and $270°$ with the $H_{ext} = 2000$ Oe. The highest T_c is observed when $\theta \sim 90°$ and the increase in T_c is ~ 30 mK. The direct obser-

vation of T_c increase supports our interpretation that the decrease of $R(\theta)$ is due to the contribution of odd-triplet superconductivity introduced in the inhomogeneous F layer. Furthermore, the magnitude of AMR in Fig. 3(a) is only about 1% while the variation in R in Fig. 3(b) is about 10%. Therefore, AMR cannot be the main reason for the variation in R near T_c. The other possible origin is the enhanced conductivity of the ferromagnetic layer. Bergeret *et al.*[23] claimed that the conductivity of the F layer can be enhanced by the penetration of the odd triplet in noncollinear system. However, the enhancement of the conductivity is along the depth direction (z axis), not in plane (xy plane). Therefore, the enhanced conductivity of the F layer cannot be an explanation of the $R(\theta)$ variation we observed.

IV. CONCLUSIONS

In conclusion, we investigated the proximity effect in an S/ES hybrid system, Nb/Py/SmFe. We found that the ES system can provide a controllable noncollinearity in the magnetizations by changing the rotating angle or the strength of external magnetic field. To avoid the stray field contribution, we rotated H_{ext} instead of sweeping H_{ext}. The angular dependence of AMR at $T > T_c$ demonstrated the noncollinear magnetization configuration of the F layer is well introduced by rotating H_{ext}. T_c increased by ~ 30 mK when maximum noncollinearity is introduced ($\theta \approx 90°$ and $H_{ext} = 2000$ Oe). We explain that our observation on $R(\theta)$ and $T_c(\theta)$ is due to the contribution of the odd-triplet condensate that exists in a noncollinear magnetization configuration generated in the soft layer of S/ES system.

*jgu@csulb.edu

†cyyou@inha.ac.kr

[1] A. I. Buzdin, Rev. Mod. Phys. **77**, 935 (2005).

[2] F. S. Bergeret, A. F. Volkov, and K. B. Efetov, Rev. Mod. Phys. **77**, 1321 (2005).

[3] J. S. Jiang, D. Davidović, D. H. Reich, and C. L. Chien, Phys. Rev. Lett. **74**, 314 (1995).

[4] J. Aarts, J. M. E. Geers, E. Bruck, A. A. Golubov, and R. Coehoorn, Phys. Rev. B **56**, 2779 (1997).

[5] L. R. Tagirov, Phys. Rev. Lett. **83**, 2058 (1999).

[6] A. I. Buzdin, A. V. Vedyayev, and N. V. Ryzhanovae, Europhys. Lett. **48**, 686 (1999).

[7] T. Löfwander, T. Champel, and M. Eschrig, Phys. Rev. B **75**, 014512 (2007).

[8] J. Y. Gu, C.-Y. You, J. S. Jiang, J. Pearson, Ya. B. Bazaliy, and S. D. Bader, Phys. Rev. Lett. **89**, 267001 (2002).

[9] C.-Y. You, Ya. B. Bazaliy, J. Y. Gu, S.-J. Oh, L. M. Litvak, and S. D. Bader, Phys. Rev. B **70**, 014505 (2004).

[10] P. Cadden-Zimansky, Ya. B. Bazaliy, L. M. Litvak, J. S. Jiang, J. Pearson, J. Y. Gu, C.-Y. You, M. R. Beasley, and S. D. Bader, Phys. Rev. B **77**, 184501 (2008).

[11] A. Y. Rusanov, S. Habraken, and J. Aarts, Phys. Rev. B **73**, 060505(R) (2006).

[12] D. Stamopoulos, E. Manios, and M. Pissas, Phys. Rev. B **75**, 014501 (2007).

[13] J. Zhu, X. Cheng, C. Boone, and I. N. Krivorotov, Phys. Rev. Lett. **103**, 027004 (2009).

[14] V. P. Mineev and K. V. Samokhin, *Introduction to Unconventional Superconductivity* (Gordon and Breach, Amsterdam, 1999).

[15] Y. Maeno, H. Hashimoto, K. Yoshida, S. Nishizaki, T. Fujita, J. G. Bednorz, and F. Lichtenberg, Nature (London) **372**, 532

(1994).

[16] I. Eremin, D. Manske, S. G. Ovchinnikov, and J. F. Annett, Ann. Phys. **13**, 149 (2004).

[17] K. Kuroki, R. Arita, and H. Aoki, Phys. Rev. B **63**, 094509 (2001).

[18] R. S. Keizer, S. T. B. Goennenwein, T. M. Klapwijk, G. Miao, G. Xiao, and A. Gupta, Nature (London) **439**, 825 (2006).

[19] A. F. Volkov, F. S. Bergeret, and K. B. Efetov, Phys. Rev. Lett. **90**, 117006 (2003).

[20] F. S. Bergeret, A. F. Volkov, and K. B. Efetov, Phys. Rev. B **68**, 064513 (2003).

[21] N. Lee, H.-Y. Choi, H. Doh, K. Char, and H.-W. Lee, Phys. Rev. B **75**, 054521 (2007).

[22] F. S. Bergeret, A. F. Volkov, and K. B. Efetov, Appl. Phys. A: Mater. Sci. Process. **89**, 599 (2007).

[23] F. S. Bergeret, A. F. Volkov, and K. B. Efetov, Phys. Rev. Lett. **86**, 4096 (2001).

[24] M. Eschrig, J. Kopu, J. C. Cuevas, and Gerd Schon, Phys. Rev. Lett. **90**, 137003 (2003).

[25] Z. Pajović, M. Božović, Z. Radović, J. Cayssol, and A. Buzdin, Phys. Rev. B **74**, 184509 (2006).

[26] M. Houzet and A. I. Buzdin, Phys. Rev. B **76**, 060504(R) (2007).

[27] Trupti S. Khaire, Mazin A. Khasawneh, W. P. Pratt, Jr., and Norman O. Birge, Phys. Rev. Lett. **104**, 137002 (2010).

[28] A. F. Volkov and K. B. Efetov, Phys. Rev. B **81**, 144522 (2010).

[29] M. Houzet and A. I. Buzdin, Phys. Rev. B **74**, 214507 (2006).

[30] Z. Yang, M. Lange, A. Volodin, R. Szymczak, and V. V. Moshchalkov, Nature Mater. **3**, 793 (2004).

[31] A. F. Volkov, A. A. Anishchanka, and K. B. Efetov, Phys. Rev. B **73**, 104412 (2006).

[32] Ya. V. Fominov, A. F. Volkov, and K. B. Efetov, Phys. Rev. B **75**, 104509 (2007).

[33] A. Yu. Rusanov, M. Hesselberth, J. Aarts, and A. I. Buzdin, Phys. Rev. Lett. **93**, 057002 (2004).

[34] L. Y. Zhu, T. Y. Chen, and C. L. Chien, Phys. Rev. Lett. **101**, 017004 (2008).

[35] E. E. Fullerton, J. S. Jiang, M. Grimsditch, C. H. Sowers, and S. D. Bader, Phys. Rev. B **58**, 12193 (1998).

[36] E. E. Fullerton, J. S. Jiang, and S. D. Bader, J. Magn. Magn. Mater. **200**, 392 (1999).

[37] Z. J. Guo, J. S. Jiang, C.-Y. You, V. K. Vlasko-Vlasov, U. Welp, J. P. Liu, and S. D. Bader, J. Appl. Phys. **93**, 8122 (2003).

[38] J. Y. Gu, J. Burgess, and C.-Y. You, J. Appl. Phys. **107**, 103918 (2010).

[39] T. R. McGuire and R. I. Potter, IEEE Trans. Magn. **11**, 1018 (1975).

[40] I. Baladié, A. Buzdin, N. Ryzhanova, and A. Vedyayev, Phys. Rev. B **63**, 054518 (2001).

[41] Ya. V. Fominov, N. M. Chtchelkatchev, and A. A. Golubov, Phys. Rev. B **66**, 014507 (2002).

[42] Ya. V. Fominov, A. A. Golubov, and M. Yu. Kupriyanov, JETP Lett. **77**, 510 (2003).

[43] M. Hübener, D. Tikhonov, I. A. Garifullin, K. Westerholt, and H. Zabel, J. Phys.: Condens. Matter **14**, 8687 (2002).

[44] C. Bell, E. J. Tarte, G. Burnell, C. W. Leung, D.-J. Kang, and M. G. Blamire, Phys. Rev. B **68**, 144517 (2003).